Acta Pharmacologica Sinica

www.nature.com/aps

ARTICLE

Identification of critical molecular pathways involved in exosome-mediated improvement of cardiac function in a mouse model of muscular dystrophy

Xuan Su[1], Yan Shen[1], Yue Jin[1], Neal L Weintraub[1] and Yao-liang Tang[1]

Duchenne muscular dystrophy (DMD) is a progressive disease characterized by skeletal muscle atrophy, respiratory failure, and cardiomyopathy. Our previous studies have shown that transplantation with allogeneic myogenic progenitor-derived exosomes (MPC-Exo) can improve cardiac function in X-linked muscular dystrophy (Mdx) mice. In the present study we explored the molecular mechanisms underlying this beneficial effect. We quantified gene expression in the hearts of two strains of Mdx mice (D2.B10-Dmd^{Mdx}/J and $Utrn^{tm1Ked}$-Dmd^{Mdx}/J). Two days after MPC-Exo or control treatment, we performed unbiased next-generation RNA-sequencing to identify differentially expressed genes (DEGs) in treated Mdx hearts. Venn diagrams show a set of 780 genes that were ≥2-fold upregulated, and a set of 878 genes that were ≥2-fold downregulated, in both Mdx strains following MPC-Exo treatment as compared with control. Gene ontology (GO) and protein-protein interaction (PPI) network analysis showed that these DEGs were involved in a variety of physiological processes and pathways with a complex connection. qRT-PCR was performed to verify the upregulated ATP2B4 and Bcl-2 expression, and downregulated IL-6, MAPK8 and Wnt5a expression in MPC-Exo-treated Mdx hearts. Western blot analysis verified the increased level of Bcl-2 and decreased level of IL-6 protein in MPC-Exo-treated Mdx hearts compared with control treatment, suggesting that anti-apoptotic and anti-inflammatory effects might be responsible for heart function improvement by MPC-Exo. Based on these findings, we believed that these DEGs might be therapeutic targets that can be explored to develop new strategies for treating DMD.

Keywords: Duchenne muscular dystrophy; cardiomyopathy; exosome; RNA-Seq; gene ontology; protein-protein interaction network; Bcl-2; IL-6

Acta Pharmacologica Sinica (2021) 42:529–535; https://doi.org/10.1038/s41401-020-0446-y

INTRODUCTION

Duchenne muscular dystrophy (DMD) is an X-linked recessive and progressive neuromuscular disease affecting approximately one per 3600 newborn boys worldwide [1]. It is caused by mutations in the gene encoding the dystrophin protein on the X chromosome [2], resulting in a series of events associated with progressive muscle dysfunction. In the absence of functional dystrophy proteins, Mauduit et al. [3] reported that 6%–9% of affected mice often develop progressive rhabdomyosarcoma, since DMD is also a tumor suppressor in sarcomas. Respiratory failure used to be the major cause of death in DMD patients [4]. However, due to the wide application of mechanical ventilation, heart failure due to cardiomyopathy has become the leading cause of patient death [5]; this is in part because therapeutic options for cardiomyopathy associated with DMD are limited [6–8].

To explore a novel treatment approach for DMD cardiomyopathy, we previously tested the effects of intramyocardial transplantation of exosomes derived from allograft myogenic progenitor cells (MPC-Exos) on cardiac function in mice with X-linked muscular dystrophy (Mdx) [9, 10]. There was a significant improvement in cardiac function two days after MPC-Exo transplantation, suggesting that allograft MPC-Exo transplantation might be an effective therapeutic approach. However, the mechanisms underlying this benefit remain unknown.

Sequencing of RNA, or RNA-Seq, is now a standard method to analyze gene expression to identify and quantify each RNA molecule in a given cell or under a specific condition [11]. It can also provide insight into the complex regulatory mechanisms underlying therapeutic interventions. Here, we performed next-generation RNA-Seq and transcriptome analysis two days after intramyocardial exosome transplantation into Mdx mice. To account for interstrain variation, we employed two different strains: D2. B10-Dmd^{Mdx}/J mice and $Utrn^{tm1Ked}$ Dmd^{Mdx}/J mice. By a combined analysis of gene expression and strain variation data, we unraveled possible molecular mechanisms involved in the improvement of cardiac function following allograft MPC-Exo transplantation in Mdx mice.

MATERIALS AND METHODS

Intramyocardial exosome transplantation

D2. B10-Dmd^{Mdx}/J mice and $Utrn^{tm1Ked}$ Dmd^{Mdx}/J mice (male; age > 10 months; and body weight (BW) > 18 g) (The Jackson Laboratory, Bar Harbor, ME, USA) were anesthetized by intraperitoneal injection

[1]Vascular Biology Center, Medical College of Georgia, Augusta University, Augusta, GA 30912, USA
Correspondence: Yao-liang Tang (yaotang@augusta.edu)

Received: 5 December 2019 Accepted: 17 May 2020
Published online: 29 June 2020

of 100 mg/kg body weight (BW) ketamine and 10 mg/kg BW xylazine. Mice were then endotracheally intubated using a 24-gauge tube and were ventilated with room air using a Harvard rodent ventilator (Inspira Advanced Safety Ventilator Model 55–7058, Holliston, MA, USA). The chest was opened via lateral thoracotomy through the fourth intercostal space, and the heart was exposed via pericardiotomy. MPC-Exos were isolated and purified as previously described [9, 10, 12, 13]. As we reported before, the purified exosomes appeared under electron micrography as round, cup-shaped vesicles; the size of each exosome is approximately 100 nm, and the zeta potential is approximately −20.81 ± 1.64 mV at 23 °C, as shown by ZetaView analysis [9, 10]. MPC-Exo (50 μg in 30 μL of PBS) or PBS (30 μL) alone (as a control) was injected intramyocardially into the left anterior wall ($n = 6$/group). The chest was closed, and the mice were allowed to recover. Animals were handled according to approved protocols and animal welfare regulations of the Institutional Animal Care and Use Committee of the Medical College of Georgia at Augusta University.

RNA extraction, mRNA-Seq library preparation, and sequencing
Two days after MPC-Exo/PBS injection, the hearts were harvested and homogenized. Total RNA was extracted by RNAzol RT (Molecular Research Center, Inc, Cincinnati, OH, USA) from the homogenates of cardiac tissue according to the manufacturer's instructions. RNA quantity and purity were assessed with a Nanodrop 2000 spectrophotometer (Thermo Scientific). Five micrograms of total RNA was used per sample to construct Illumina sequencing libraries using a Lexogen's SENSE^{TM} mRNA-Seq Kit V2 according to the manufacturer's instructions. mRNA libraries were sequenced on an Illumina Hi-Seq 4000 platform based on sequencing by synthesis with 50 bp single-end reads.

mRNA transcriptome data analysis
Primary sequencing data produced on a Illumina Hi-Seq 4000 platform were analyzed by ArrayStar Software (DNASTAR, Inc., Madison, WI, USA) to generate heat maps of selected genes of interest. A fold change ≥2 (log2 ratio > 1) was set to identify differentially expressed genes (DEGs). To further process the data, DAVID Bioinformatics Resources 6.8 (https://david.ncifcrf.gov/) [14] was used to perform Gene Ontology (GO) enrichment analysis.

Generation of the protein-protein interaction (PPI) network
A visual analytics online software program (NetworkAnalyst, http://www.networkanalyst.ca/) [15] updated on 2019-07-30 was applied to analyze the DEGs and construct PPI networks. The 780 common upregulated and 878 common downregulated DEGs were displayed and uploaded together into a list with official gene symbols. STRING Interactome was selected as the PPI database with confidence scores ranging from medium (400) to high (1000), in which 900 was set as the cutoff for the analysis. The seeds were mapped to the corresponding molecular interaction database, and subnetworks with at least three nodes were identified. The degree of each node was calculated based on its number of connections to other nodes. In the network, the area of an individual node indicates the degree, and the color represents the expression.

qRT-PCR analysis for the validation of RNA-Seq data
Quantitative real-time PCR (qRT-PCR) was performed to validate the transcriptome sequencing data. Total RNA isolated for RNA sequencing was used in qRT-PCR assays. Reverse transcription was performed with 1 μg of total RNA using RevertAid First Strand cDNA Synthesis kits (Thermo Scientific). The cDNA was used to perform qRT-PCR on a CFX96 Touch Real-Time PCR Detection System (Bio-Rad Laboratories) using PowerUp SYBR Green Master Mix (Thermo Fisher). Amplification was performed at 50 °C for 2 min and 95 °C for 2 min, which was followed by 50 cycles of 95 °C for 15 s and 60 °C for 1 min; the primers used are listed in Table 1. The relative gene expression levels were first normalized to β-actin and then were calculated using the comparative cycle threshold method (ΔΔCt) [16].

Table 1. Primer list.

Gene	Sequence (5′-3′)
B-actin	FWD AGAGCATAGCCCTCGTAGAT
B-actin	REV GCTGTGCTGTCCCTGTATG
VDR	FWD GTGGCAGCCAAGACTACAAATA
VDR	REV CTCATGGAGGTTCAGCTTCTTC
ATP2B4	FWD GGTCAGGTCATCTCTGCAATAC
ATP2B4	REV CATCTCGGCAAGGTCAATCT
Bcl-2	FWD TTGTGGCCTTCTTTGAGTTCGGTG
Bcl-2	REV ATGCCGGTTCAGGTACTCAGTCAT
IL-6	FWD ATCCAGTTGCCTTCTTGGGACTGA
IL-6	REV TAAGCCTCCGACTTGTGAAGTGGT
MAPK8	FWD GATGAGAGGGAGCACACAATAG
MAPK8	REV TGCTGCACCTGTGCTAAA
Wnt5a	FWD GCTAGAGAAAGGGAACGAATCC
Wnt5a	REV CCAGACACTCCATGACACTTAC

Western blotting assay
The Bcl-2, IL-6, Wnt5a, and MAPK8 genes verified by qRT-PCR were selected for Western blot analysis, as previously described [17, 18]. Briefly, hearts were lysed in RIPA buffer (Alfa Aesar). Proteins (30 μg) were resolved on 10% SDS-polyacrylamide gels and then were transferred onto Odyssey® nitrocellulose membranes (LI-COR Biosciences). The membranes were blocked with Odyssey blocking buffer (LI-COR Biosciences) and then were probed with rabbit anti-Bcl-2 (1:250; Santa Cruz), rat anti-IL-6 (1:1000; R&D Systems), goat anti-Wnt5a (1:1000; R&D Systems), rabbit anti-MAPK8 (1:1000, Cell Signaling), and mouse anti-GAPDH (1:5000, Millipore) at 4 °C overnight. After washing with 1× TBST, the membranes were incubated for 1 h at room temperature with IRDye 680 goat anti-rabbit IgG and IRDye 800 goat anti-mouse IgG (1:10,000, LI-COR Biosciences). The probed blots were scanned using an Odyssey infrared imager (LI-COR Biosciences).

Statistical analysis
The results are indicated as the mean ± standard error of the mean (SEM). Unpaired Student's *t*-tests were used to compare two groups. A value of $P < 0.05$ was considered statistically significant. Statistical analyses were conducted with GraphPad Prism 7.0 software.

RESULTS

Transcriptome analysis and DEG identification
In the hearts of D2. B10-Dmd^{Mdx}/J mice, a total of 6812 genes were differentially expressed in the MPC-Exo group compared to the control, with 2954 genes upregulated (Fig. 1a) and 3858 genes downregulated (Fig. 1d). In the hearts of Utrn^{tm1Ked} Dmd^{Mdx}/J mice, 11800 DEGs were detected in the MPC-Exo group compared to the control, with 5906 upregulated genes (Fig. 1b) and 5894 downregulated genes (Fig. 1e). Venn diagrams showed an overlapping pattern of gene sets with ≥2-fold upregulated or downregulated genes in MPC-Exo-treated D2. B10-Dmd^{Mdx}/J and Utrn^{tm1Ked} Dmd^{Mdx}/J mice. Only 780 genes were commonly upregulated, and 878 genes were commonly downregulated in both strains of mice, as illustrated in the Venn diagram in Fig. 1c and f; the remaining genes were differentially regulated in only one strain of Mdx mice.

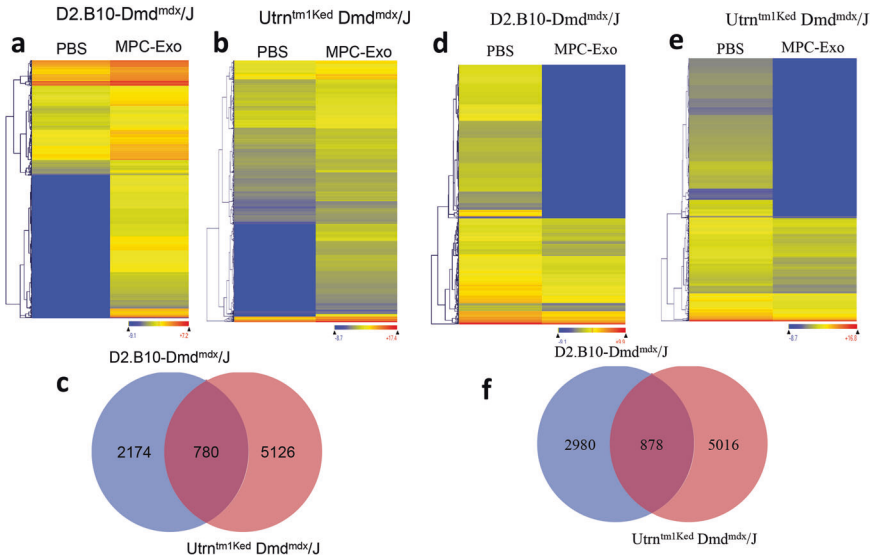

Fig. 1 Transcriptome analysis and DEG identification. a Heatmaps of upregulated gene expression in MPC-Exos versus PBS-treated D2. B10-Dmd^{Mdx}/J mice. **b** Heatmaps of upregulated gene expression in MPC-Exo versus PBS-treated Utrn^{tm1Ked} Dmd^{Mdx}/J mice. **c** Overlap of upregulated DEGs identified in the two strains of MDX mice. **d** Heatmaps of downregulated gene expression in MPC-Exos versus PBS-treated D2. B10-Dmd^{Mdx}/J mice. **e** Heatmaps of downregulated gene expression in MPC-Exo versus PBS-treated Utrn^{tm1Ked} Dmd^{Mdx}/J mice. **f** Overlap of downregulated DEGs identified in the two strains of MDX mice.

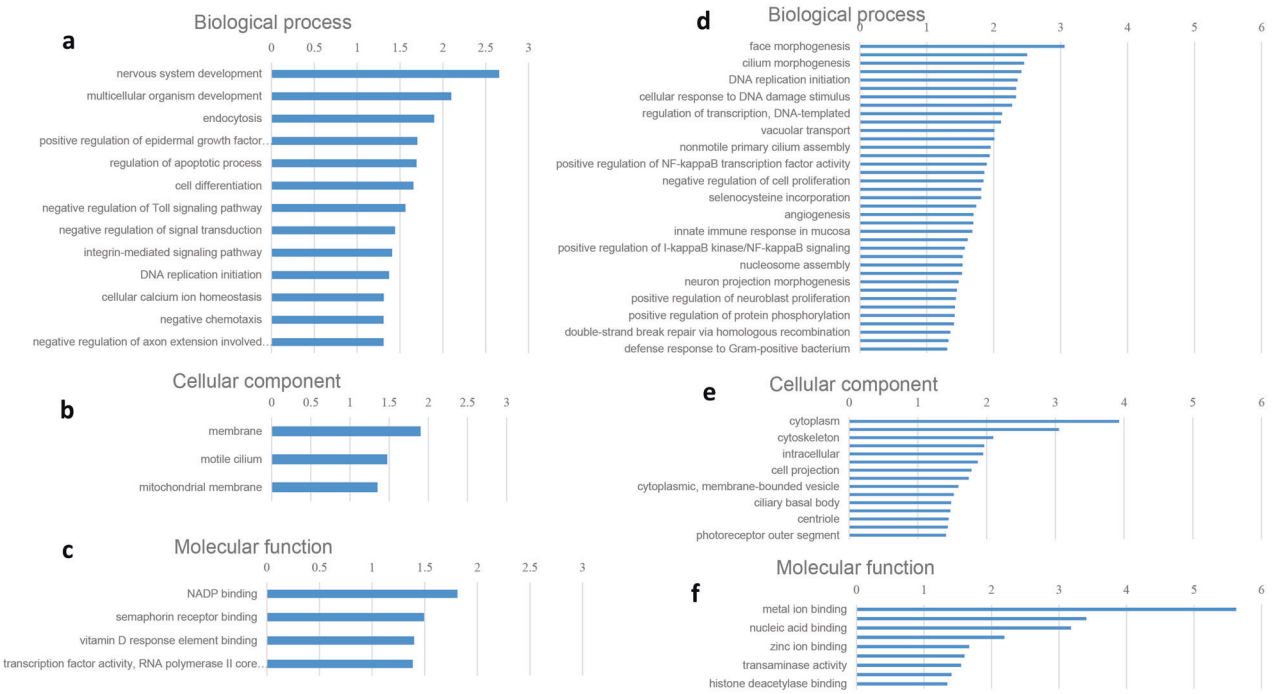

Fig. 2 Gene ontology (GO) analysis. The significantly enriched GO terms that corresponded to coding gene functions of (**a**–**c**) upregulated and (**d**–**f**) downregulated DEGs are listed. **a**, **d** biological process; **b**, **e** cellular component; **c**, **f** molecular function. The enrichment score indicates the enrichment score value of the GO item, equivalent to -log10(*P*-value).

Annotation and enrichment of DEGs

To determine the biological implications of this data set, GO analysis was performed to determine the gene and gene product enrichment in the following categories: biological process (BP), cellular component (CC), and molecular function (MF). In the GO analysis, the upregulated and downregulated DEGs were analyzed separately, and significantly enriched GO networks were identified (Fig. 2) by setting the *P*-value < 0.05. In the category of BP, modulation of the apoptotic process and cellular calcium ion homeostasis were identified as significantly enriched networks associated with the upregulated DEGs. Furthermore, positive regulation of the transcription factor NF-kappaB activity was identified in downregulated DEGs. In the category of CC, the category of membrane items was the abundantly upregulated in DEGs, while DEGs involved in the cytoplasm were significantly downregulated. Among the MF items, the most significantly enriched function of the upregulated DEGs was NADP binding, and the highest proportion of downregulated DEGs was distributed in metal ion binding.

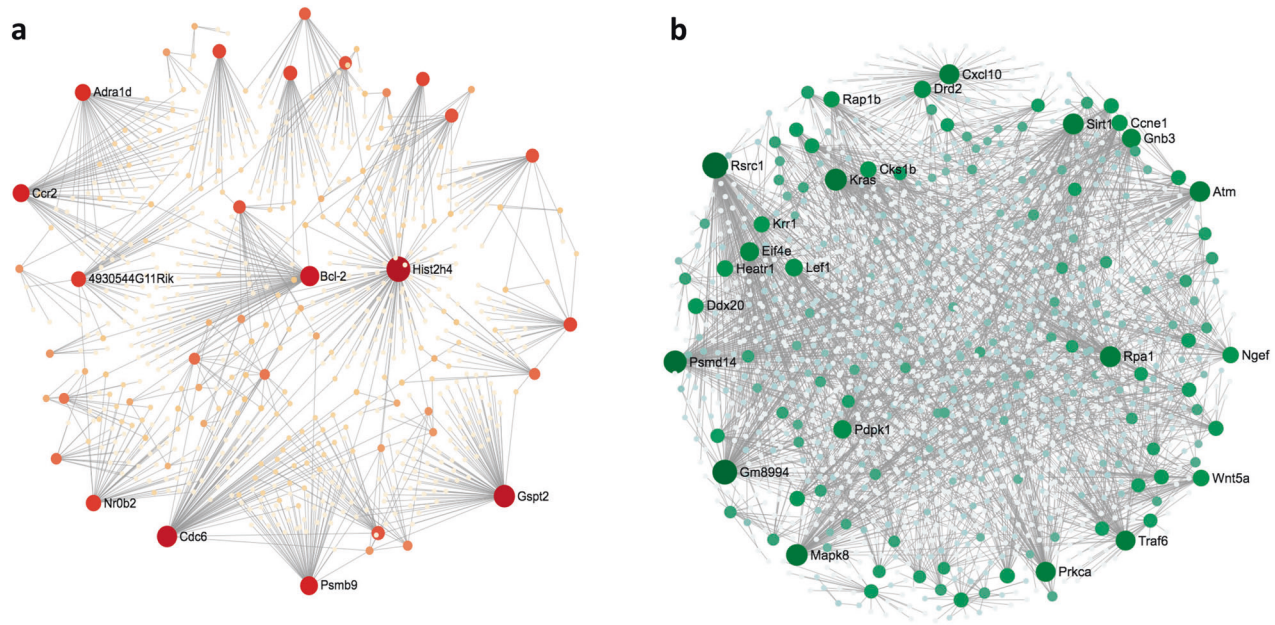

Fig. 3 The constructed PPI network of the upregulated and downregulated differentially expressed genes. a Upregulated PPI network analysis of DEGs in MPC-Exo-treated hearts compared to PBS-treated control hearts. **b** The downregulated PPI network analysis of DEGs in MPC-Exo-treated hearts compared to control hearts. The nodes represent proteins, and the edges represent the interaction of proteins.

Table 2. The information of genes selected to verify RNA sequencing analysis.

Gene	Function	Expression[a]
VDR	Cellular calcium ion homeostasis	Up
ATP2B4	Cellular calcium ion homeostasis	Up
Bcl-2	Apoptosis	Up
IL-6	Inflammation and apoptosis	Down
MAPK8	JNK cascade	Down
Wnt5a	Inflammation	Down

[a]This expression indicated the expression changes in MPC-Exo treatment by RNA-Seq.

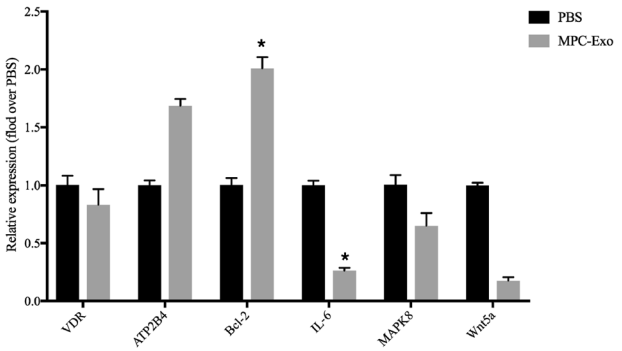

Fig. 4 qRT-PCR verification of the expression levels of 6 genes in Utrn^{tm1Ked} Dmd^{Mdx}/J mice treated with PBS or MPC-Exo. The amount of mRNA was normalized using β-actin, and the relative expression was normalized to the levels observed after PBS treatment. The results are shown as the mean with SEM (*$P < 0.05$ vs. PBS, $n = 3$).

The PPI network of DEGs

Interactions between the identified DEGs were revealed by constructing a PPI network. As shown in Fig. 3a, the upregulated PPI network included 760 nodes and 912 edges. According to degree levels, the top five hub nodes were Hist2h4, Gspt2, Cdc6, Bcl-2, and Psmb9. Meanwhile, 1817 nodes and 2661 edges were included in the downregulated PPI network (Fig. 3b), and the top five hub nodes were Rsrc1, Gm8994, Psmd14, Kras, Mapk8 and Wnt5a.

Critical gene selection and validation by qRT-PCR and Western blot

DEGs that regulated representative functions or those whose expression profiles were extremely altered in response to MPC-Exo treatment were selected (Table 2) for verification of the RNA sequencing analysis using qRT-PCR. Bcl-2 was related to the regulation of the apoptotic process, ATP2B4 and VDR were associated with cellular calcium ion homeostasis, Wnt5a and IL-6 corresponded to inflammation and apoptosis, and MAPK8 was correlated to the JNK cascade. We confirmed that Bcl2 and ATP2B4 were upregulated, while IL-6, Wnt5a, and MAPK8 were downregulated in Utrn^{tm1Ked} Dmd^{Mdx}/J mice with MPC-Exo treatment compared to the control (Fig. 4). Except for VDR, the qRT-PCR results and RNA-Seq data were consistent, indicating that the transcriptome data were reliable. We further measured the protein levels of four genes by Western blot, as shown in Fig. 5. MPC-Exo treatment significantly increased Bcl-2 protein levels ($P < 0.05$) and significantly decreased IL-6 levels ($P < 0.001$) in Mdx hearts compared to control treatment; however, MPC-Exo treatment did not significantly reduce Wnt5a protein levels or increase total MAPK8 protein levels in Mdx hearts, suggesting that anti-apoptotic and anti-inflammatory effects might be responsible for heart function improvement by MPC-Exo.

DISCUSSION

Si1nce mice with Mdx show muscle pathophysiological properties that are similar to those of patients with DMD, the Mdx mouse model has been widely used in DMD studies [19–21]. The aged Mdx mouse displays progressive fibrosis in most skeletal muscles, respiratory muscles, and heart muscles, with features including motor dysfunction, respiratory compromise, and cardiomyopathy [7]. Adult C57BL/10-Mdx mice do not exhibit key features of human

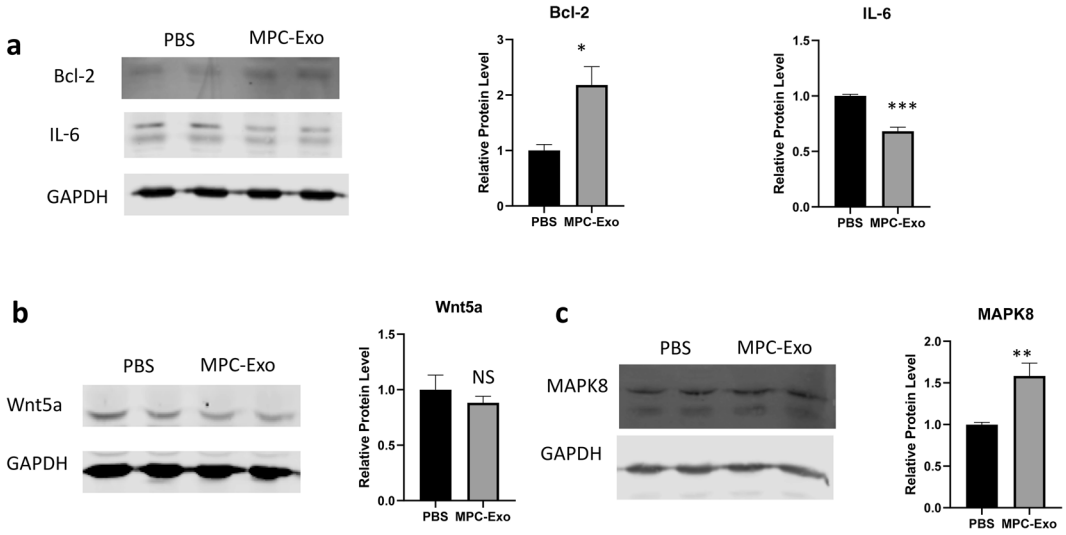

Fig. 5 Western blot verification of the protein levels of Bcl-2, IL-6, Wnt5a, and MAPK8 in Utrn^{tm1Ked} Dmd^{Mdx}/J mice treated with PBS or MPC-Exo. The amount of protein was normalized using GAPDH, and the relative expression was normalized to the levels observed after PBS treatment. The results are shown as the mean with SEM (*$P < 0.05$ **$P < 0.01$, and ***$P < 0.001$ vs PBS, $n = 3$ or 4).

DMD, including increased muscle fat accumulation and fibrosis, insufficient muscle fiber regeneration, and reduced muscle mass. In the present study, we chose two superior Mdx mouse models, D2. B10-Dmd^{Mdx}/J and Utrntm1Ked-Dmd^{Mdx}/J mice, as recipient mice for MPC-Exos, since both recapitulate human characteristics of DMD myopathology. We subjected these two strains of Mdx mice to intramyocardial MPC-Exo treatment and used unbiased next-generation sequencing and bioinformatic approaches to investigate the molecular mechanisms whereby MPC-Exos improve cardiac function in Mdx mice. Our findings might provide new targets for the future therapy of DMD cardiomyopathy.

We identified 1658 DEGs, of which 780 were upregulated and 878 were downregulated after MPC-Exo treatment in both strains of Mdx mice relative to controls. Based on these DEGs, we performed GO enrichment analysis to identify the genetic framework and analyzed the gene product activities in terms of BP, MF, and CC. In BP analysis of regulated DEGs, we observed that cellular calcium ion homeostasis and regulation of the apoptotic process were two of the most critical processes modulated by MPC-Exo treatment.

Among the upregulated DEGs, ATP2B4 was implicated in the process of cellular calcium ion homeostasis [22]. Encoding the plasma membrane calcium ATPase (PMCA) isoform 4, ATP2B4 is a member of the PMCA family, which extrudes Ca^{2+} from the cell and is involved in the maintenance of intracellular free calcium levels and Ca^{2+} signaling [23]. Heart failure was associated with reduced expression of ATP2B4, and cardiac-specific overexpression of ATP2B4 preserved cardiac function with increased contractility in mouse models of myocardial ischemia-reperfusion injury [24]. Thus, the upregulation of ATP2B4 resulting from MPC-Exo treatment may contribute to the improvement of cardiac function in Mdx mice.

Additionally, we found several upregulated DEGs involved in the regulation of apoptosis, such as Bcl-2, a crucial anti-apoptotic gene, which was also one of the top five hub nodes in the upregulated PPI network. Dilated cardiomyopathy due to cardiomyocyte loss is one of the significant causes of lethality in late-stage DMD patients [25]. Several studies demonstrated that overexpression of Bcl-2 in the heart diminished apoptotic cells, reduced infarct size, and improved recovery of cardiac function after myocardial ischemia-reperfusion injury in mice [26, 27], suggesting that Bcl-2 provided myocardial protection possibly by blocking p53-mediated apoptosis [28] and inhibiting consumption of ATP generated in cardiomyocytes [29]. A previous study demonstrated a significant decrease in Bcl-2 protein in patients with DMD compared to controls, suggesting that Bcl-2 is involved in muscle atrophy and degeneration [30]. Therefore, elevated expression of Bcl-2 might contribute to the improved cardiac function in MPC-Exo-treated Mdx mice by providing anti-apoptotic effects in cardiomyocytes.

IL-6 levels were reported to be significantly increased in patients with DMD and in the Mdx mouse model [31], and it was identified as one of the significantly downregulated genes among numerous DEGs. The cellular response to IL-6 in the heart has been well characterized. IL-6 can play a protective role in the short term of the acute response, such as myocardial infarction [32, 33], while long-term IL-6 signaling plays a causal role in chronic inflammation and progression of heart failure [34, 35]. Pelosi et al. [31] reported that inhibition of IL-6 activity by using IL-6 antagonism can counteract necrosis and improve the muscle functional performance of Mdx mice. Since DMD is a chronic and progressive disease, decreased IL-6 expression following MPC-Exo treatment would likely provide a benefit to Mdx mice. Furthermore, in recent years, IL-6 has been linked to the maintenance and propagation of the senescence-associated secretory phenotype (SASP) response [36, 37]. Downregulation of IL-6 expression in the heart might thus prevent the senescence of cardiac cells, including cardiomyocytes, endothelial cells, smooth muscle cells, and fibroblasts, which would delay the progression of cardiac dysfunction in Mdx mice with increasing age [38].

MAPK8 (mitogen-activated protein kinase 8), also known as JNK1 (c-Jun N-terminal kinase 1), was identified to be significantly downregulated following MPC-Exo treatment in our study and was one of the top five hub nodes in the downregulated PPI network. It is a mitogen-activated protein kinase that plays an essential role in the pathogenesis of cardiac and vascular disease [39]. Activation of MAPK8 has been observed in human heart failure in a previous study [40], and transgenic activation of the JNK pathway in the mouse heart has been demonstrated to result in lethal restrictive cardiomyopathy with extracellular matrix remodeling [41]. In addition, JNK has been linked to various pathways promoting cardiac remodeling, such as matrix metalloproteinases (MMP) [42], β-adrenergic signaling [43], and reactive oxygen species (ROS) signaling [44]. In our study, we observed that MAPK8 was downregulated at the mRNA level, but it was not downregulated at the protein level. The inconsistency between MAPK8 mRNA and protein levels indicated posttranscriptional regulation, such as microRNA regulation.

Wnt5a (Wnt Family Member 5A), a noncanonical ligand of the Wnt pathway, was also detected as a significantly downregulated node in the PPI network. Wnt5a was found to be elevated in serum and failing myocardium in patients with heart failure, and it is associated with disease progression [45] and adverse outcomes [46]. Experimental studies identified fibroblasts as the primary source of Wnt5a; moreover, Wnt5a induced inflammatory and profibrotic responses in the lung and cardiac fibroblasts [45, 47]. In our study, we observed that Wnt5a mRNA was significantly reduced after MPC-Exo treatment, but the Wnt5a protein was only slightly reduced. Our previous studies showed that exosomes from cardiac mesenchymal stem cells reduced H3K27 demethylase UTX expression, thus increasing the protein level of H3K27me3 in treated mouse cardiomyocytes [12]. H3K27me3 is a suppressor marker that inhibits transcriptional gene expression. This mechanism might explain the significant reduction in Wnt5a transcription after MPC-Exo treatment. The slight decrease in the Wnt5a protein level may be due to undegraded, previously synthesized Wnt5a protein.

In conclusion, using next-generation sequencing techniques, this study identified candidate genes and pathways that may be involved in cardiac function improvement following allograft MPC-Exo transplantation in DMD mice. Studying the relationships among these DEGs may facilitate a deeper understanding of the potential mechanisms of the beneficial effects of allograft MPC-Exo transplantation in MDX mice. We suggest that these DEGs may yield insight into the cardiomyopathy associated with DMD, and using these DEGs as therapeutic targets may help develop a new treatment strategy for patients with DMD.

The aim of this study was to investigate the mechanisms behind transient improvement in heart function in Mdx mice after allogeneic MPC-Exo treatment. Through unbiased high-throughput RNA-seq, bioinformatics analysis of DEGs, PPI based on String analysis followed by qRT-PCR and Western blot validation of major DEGs, we found that a set of anti-apoptotic genes were upregulated, and a set of inflammatory genes were downregulated, suggesting that anti-apoptotic and anti-inflammatory effects might contribute to the improvement in heart function after MPC-Exo treatment of Mdx mice. There are several limitations of this study: (1) Exosomes can only transiently relieve symptoms in degenerative diseases, such as DMD. To achieve a robust long-term improvement of cardiac function, using CRISPR-Cas9 technology to correct DMD mutation might be an ideal strategy [48]; (2) RNA-seq only provided high-throughput mRNA information, and further information about microRNAs or protein profiles might provide additional interesting information accounting for improvement of cardiac function; (3) Further functional tests of a set of DEGs using knockdowns and rescue experiments can help us prove the importance of Bcl-2 and IL-6 in MPC-Exo-mediated cardioprotection of Mdx mice; (4) RNA-seq analysis of heart tissue cannot define the effects of MPC-Exo on individual cell populations in heart, including cardiomyocytes, smooth muscle cells, endothelial cells, cardiac progenitor cells, and cardiac fibroblasts, but single-cell RNA-seq could provide this interesting information.

ACKNOWLEDGEMENTS

This study was funded by grants HL124097 and HL126949 (NLW), HL134354 (YLT and NLW), and HL086555 (YLT) from the National Institutes of Health.

AUTHOR CONTRIBUTIONS

YLT designed the research; XS, YS, YJ performed the research; YLT and XS analyzed the data; and XS, NLW and YLT wrote the paper.

ADDITIONAL INFORMATION

Conflict of interest: The authors declare that they have no conflict of interest.

REFERENCES

1. Chung J, Smith AL, Hughes SC, Niizawa G, Abdel-Hamid HZ, Naylor EW, et al. Twenty-year follow-up of newborn screening for patients with muscular dystrophy. Muscle Nerve. 2016;53:570–8.
2. Hoffman EP, Brown RH Jr, Kunkel LM. Dystrophin: the protein product of the Duchenne muscular dystrophy locus. Cell. 1987;51:919–28.
3. Mauduit O, Delcroix V, Lesluyes T, Perot G, Lagarde P, Lartigue L, et al. Recurrent DMD Deletions Highlight Specific Role of Dp71 Isoform in Soft-Tissue Sarcomas. Cancers (Basel). 2019;11:922.
4. Fukunaga H, Sonoda Y, Atsuchi H, Osame M. Respiratory failure and its care in Duchenne muscular dystrophy. Rinsho Shinkeigaku. 1991;31:154–8.
5. Kuno A, Horio Y. SIRT1: a novel target for the treatment of muscular dystrophies. Oxid Med Cell Longev. 2016;2016:6714686.
6. Eagle M, Baudouin SV, Chandler C, Giddings DR, Bullock R, Bushby K. Survival in Duchenne muscular dystrophy: improvements in life expectancy since 1967 and the impact of home nocturnal ventilation. Neuromuscul Disord. 2002;12:926–9.
7. McNally EM, Kaltman JR, Benson DW, Canter CE, Cripe LH, Duan D, et al. Contemporary cardiac issues in Duchenne muscular dystrophy. Working Group of the National Heart, Lung, and Blood Institute in collaboration with Parent Project Muscular Dystrophy. Circulation. 2015;131:1590–8.
8. Kamdar F, Garry DJ. Dystrophin-deficient cardiomyopathy. J Am Coll Cardiol. 2016;67:2533–46.
9. Su X, Jin Y, Shen Y, Ju C, Cai J, Liu Y, et al. Exosome-derived dystrophin from allograft myogenic progenitors improves cardiac function in duchenne muscular dystrophic mice. J Cardiovasc Transl Res. 2018;11:412–9.
10. Su X, Shen Y, Jin Y, Jiang M, Weintraub N, Tang Y. Purification and transplantation of myogenic progenitor cell derived exosomes to improve cardiac function in duchenne muscular dystrophic mice. J Vis Exp. 2019. https://doi.org/10.3791/59320.
11. Hrdlickova R, Toloue M, Tian B. RNA-Seq methods for transcriptome analysis. Wiley interdisciplinary reviews. RNA. 2017. https://doi.org/10.1002/wrna.1364.
12. Ruan XF, Li YJ, Ju CW, Shen Y, Lei W, Chen C, et al. Exosomes from Suxiao Jiuxin pill-treated cardiac mesenchymal stem cells decrease H3K27 demethylase UTX expression in mouse cardiomyocytes in vitro. Acta Pharmacol Sin. 2018;39:579–86.
13. Ruan XF, Ju CW, Shen Y, Liu YT, Kim IM, Yu H, et al. Suxiao Jiuxin pill promotes exosome secretion from mouse cardiac mesenchymal stem cells in vitro. Acta Pharmacol Sin. 2018;39:569–78.
14. Huang da W, Sherman BT, Lempicki RA. Systematic and integrative analysis of large gene lists using DAVID bioinformatics resources. Nat Protoc. 2009;4:44–57.
15. Zhou G, Soufan O, Ewald J, Hancock REW, Basu N, Xia J. NetworkAnalyst 3.0: a visual analytics platform for comprehensive gene expression profiling and meta-analysis. Nucleic Acids Res. 2019;47:W234–w41.
16. Schmittgen TD, Livak KJ. Analyzing real-time PCR data by the comparative C(T) method. Nat Protoc. 2008;3:1101–8.
17. Su X, Jin Y, Shen Y, Kim IM, Weintraub NL, Tang Y. RNAase III-type enzyme dicer regulates mitochondrial fatty acid oxidative metabolism in cardiac mesenchymal stem cells. Int J Mol Sci. 2019;20:5554.
18. Chen Z, Su X, Shen Y, Jin Y, Luo T, Kim IM, et al. MiR322 mediates cardioprotection against ischemia/reperfusion injury via FBXW7/notch pathway. J Mol Cell Cardiol. 2019;133:67–74.
19. Li D, Long C, Yue Y, Duan D. Sub-physiological sarcoglycan expression contributes to compensatory muscle protection in mdx mice. Hum Mol Genet. 2009;18:1209–20.
20. Bostick B, Yue Y, Long C, Duan D. Prevention of dystrophin-deficient cardiomyopathy in twenty-one-month-old carrier mice by mosaic dystrophin expression or complementary dystrophin/utrophin expression. Circ Res. 2008;102:121–30.
21. Rafael-Fortney JA, Chimanji NS, Schill KE, Martin CD, Murray JD, Ganguly R, et al. Early treatment with lisinopril and spironolactone preserves cardiac and skeletal muscle in Duchenne muscular dystrophy mice. Circulation. 2011;124:582–8.
22. Gardina PJ, Clark TA, Shimada B, Staples MK, Yang Q, Veitch J, et al. Alternative splicing and differential gene expression in colon cancer detected by a whole genome exon array. BMC Genomics. 2006;7:325.
23. Cartwright EJ, Oceandy D, Austin C, Neyses L. Ca^{2+} signalling in cardiovascular disease: the role of the plasma membrane calcium pumps. Sci China Life Sci. 2011;54:691–8.
24. Sadi AM, Afroze T, Siraj MA, Momen A, White-Dzuro C, Zarrin-Khat D, et al. Cardiac-specific inducible overexpression of human plasma membrane Ca^{2+} ATPase 4b is cardioprotective and improves survival in mice following ischemic injury. Clin Sci (Lond). 2018;132:641–54.
25. Lin B, Li Y, Han L, Kaplan AD, Ao Y, Kalra S, et al. Modeling and study of the mechanism of dilated cardiomyopathy using induced pluripotent stem cells derived from individuals with Duchenne muscular dystrophy. Dis Models Mechanisms. 2015;8:457–66.
26. Brocheriou V, Hagege AA, Oubenaissa A, Lambert M, Mallet VO, Duriez M, et al. Cardiac functional improvement by a human Bcl-2 transgene in a mouse model of ischemia/reperfusion injury. J Gene Med. 2000;2:326–33.

27. Imahashi K, Schneider MD, Steenbergen C, Murphy E. Transgenic expression of Bcl-2 modulates energy metabolism, prevents cytosolic acidification during ischemia, and reduces ischemia/reperfusion injury. Circ Res. 2004;95:734–41.
28. Kirshenbaum LA, de Moissac D. The bcl-2 gene product prevents programmed cell death of ventricular myocytes. Circulation. 1997;96:1580–5.
29. Gustafsson AB, Gottlieb RA. Bcl-2 family members and apoptosis, taken to heart. Am J Physiol Cell Physiol. 2007;292:C45–51.
30. Abdel-Salam E, Abdel-Meguid I, Korraa SS. Markers of degeneration and regeneration in Duchenne muscular dystrophy. Acta Myol. 2009;28:94–100.
31. Pelosi L, Berardinelli MG, De Pasquale L, Nicoletti C, D'Amico A, Carvello F, et al. Functional and morphological improvement of dystrophic muscle by interleukin 6 receptor blockade. EBioMedicine. 2015;2:285–93.
32. Smart N, Mojet MH, Latchman DS, Marber MS, Duchen MR, Heads RJ. IL-6 induces PI3-kinase and nitric oxide-dependent protection and preserves mitochondrial function in cardiomyocytes. Cardiovasc Res. 2006;69:164–77.
33. Gwechenberger M, Mendoza LH, Youker KA, Frangogiannis NG, Smith CW, Michael LH, et al. Cardiac myocytes produce interleukin-6 in culture and in viable border zone of reperfused infarctions. Circulation. 1999;99:546–51.
34. Hirota H, Izumi M, Hamaguchi T, Sugiyama S, Murakami E, Kunisada K, et al. Circulating interleukin-6 family cytokines and their receptors in patients with congestive heart failure. Heart Vessels. 2004;19:237–41.
35. Fontes JA, Rose NR, Cihakova D. The varying faces of IL-6: From cardiac protection to cardiac failure. Cytokine. 2015;74:62–8.
36. Coppe JP, Desprez PY, Krtolica A, Campisi J. The senescence-associated secretory phenotype: the dark side of tumor suppression. Annu Rev Pathol. 2010;5:99–118.
37. Ortiz-Montero P, Londono-Vallejo A, Vernot JP. Senescence-associated IL-6 and IL-8 cytokines induce a self- and cross-reinforced senescence/inflammatory milieu strengthening tumorigenic capabilities in the MCF-7 breast cancer cell line. Cell Commun Signal. 2017;15:17. https://doi.org/10.1186/s12964-017-0172-3.
38. Katsuumi G, Shimizu I, Yoshida Y, Minamino T. Vascular senescence in cardiovascular and metabolic diseases. Front Cardiovasc Med. 2018;5:18.
39. Rose BA, Force T, Wang Y. Mitogen-activated protein kinase signaling in the heart: angels versus demons in a heart-breaking tale. Physiol Rev. 2010;90:1507–46.
40. Muslin AJ. MAPK signalling in cardiovascular health and disease: molecular mechanisms and therapeutic targets. Clin Sci (Lond). 2008;115:203–18.
41. Petrich BG, Eloff BC, Lerner DL, Kovacs A, Saffitz JE, Rosenbaum DS, et al. Targeted activation of c-Jun N-terminal kinase in vivo induces restrictive cardiomyopathy and conduction defects. J Biol Chem. 2004;279:15330–8.
42. Siwik DA, Kuster GM, Brahmbhatt JV, Zaidi Z, Malik J, Ooi H, et al. EMMPRIN mediates beta-adrenergic receptor-stimulated matrix metalloproteinase activity in cardiac myocytes. J Mol Cell Cardiol. 2008;44:210–7.
43. Fan GC, Yuan Q, Song G, Wang Y, Chen G, Qian J, et al. Small heat-shock protein Hsp20 attenuates beta-agonist-mediated cardiac remodeling through apoptosis signal-regulating kinase 1. Circ Res. 2006;99:1233–42.
44. Anilkumar N, Sirker A, Shah AM. Redox sensitive signaling pathways in cardiac remodeling, hypertrophy and failure. Front Biosci (Landmark Ed). 2009;14:3168–87.
45. Abraityte A, Vinge LE, Askevold ET, Lekva T, Michelsen AE, Ranheim T, et al. Wnt5a is elevated in heart failure and affects cardiac fibroblast function. J Mol Med (Berl, Ger). 2017;95:767–77.
46. Abraityte A, Lunde IG, Askevold ET, Michelsen AE, Christensen G, Aukrust P, et al. Wnt5a is associated with right ventricular dysfunction and adverse outcome in dilated cardiomyopathy. Sci Rep. 2017;7:3490.
47. Newman DR, Sills WS, Hanrahan K, Ziegler A, Tidd KM, Cook E, et al. Expression of WNT5A in idiopathic pulmonary fibrosis and its control by TGF-beta and WNT7B in human lung fibroblasts. J Histochem Cytochem. 2016;64:99–111.
48. Jin Y, Shen Y, Su X, Weintraub N, Tang Y. CRISPR/Cas9 technology in restoring dystrophin expression in iPSC-derived muscle progenitors. J Vis Exp. 2019. https://doi.org/10.3791/59432.